Polymer 53 (2012) 2152–2161

Contents lists available at SciVerse ScienceDirect

Polymer

journal homepage: www.elsevier.com/locate/polymer

Modeling the kinetics of water transport and hydroexpansion in a lignocellulose-reinforced bacterial copolyester

Wil V. Srubar III [a,*], Curtis W. Frank [b], Sarah L. Billington [a]

[a] Department of Civil and Environmental Engineering, Stanford University, Stanford, CA 94305, USA
[b] Department of Chemical Engineering, Stanford University, Stanford, CA 94305, USA

ARTICLE INFO

Article history:
Received 30 November 2011
Received in revised form
13 March 2012
Accepted 20 March 2012
Available online 30 March 2012

Keywords:
Biopolymeric composites
Chemical compatibilization
Fickian diffusion

ABSTRACT

The governing kinetic behavior of water transport in a biopolymeric composite material derived from poly(β-hydroxybutyrate)-*co*-poly(β-hydroxyvalerate) and lignocellulosic wood flour were investigated along with the influence of temperature, wood flour content, and chemical modification (silane, maleic anhydride) on polymer and composite diffusivity. The water absorption process in both untreated and treated composites was found to follow the kinetics of Fickian diffusion theory. Diffusion coefficients for neat polymer and composite samples were experimentally determined, and the thermodynamics of diffusive water transport were observed to exhibit Arrhenius rate-law behavior. A model for predicting equilibrium moisture content in wood-polymer composites is presented and substantiated by obtained results and cited experimental data. Isodiffusion plots are presented to evaluate the effectiveness of chemical modifications, which were found to reduce the rates of water uptake. Both in- and out-of-plane dimensional changes were monitored during the absorption process, permitting the determination of moisture-dependent hydroexpansion coefficients.

1. Introduction

Polymers and composites from renewable resources have attracted increased interest in recent years due to rising concerns over the proliferation of non-biodegradable plastics in the environment and a consciousness that petroleum-based resources are both limited and finite. Natural alternatives are being sought for replacements to conventional composite materials in the automotive, packaging, and construction industries where virgin polyolefin thermoplastics and inorganic reinforcements such as glass, aramid, and carbon fibers have traditionally dominated the market [1].

Promising biorenewable polymers include starch- and cellulose-based resins, poly(lactic acids) (PLAs), and poly(hydroxyalkanoates) (PHAs), which are the focus of the work presented here. PHAs are a family of aliphatic biodegradable polyesters synthesized via bacterial fermentation under nutrient-limited conditions [2]. PHAs are of interest because they (1) are biodegradable, (2) can be microbially synthesized using natural carbon sources, including sugar and methane, and (3) are highly crystalline and hydrophobic, demonstrating good mechanical properties similar to conventional polyolefin thermoplastics used in commercial wood plastic composites. The most commonly synthesized and well-characterized PHA is poly(β-hydroxybutyrate) (PHB), a highly crystalline, hydrophobic thermoplastic typically used in niche biomedical and tissue engineering applications. Poly(β-hydroxybutyrate)-*co*-poly(β-hydroxyvalerate) (PHBV), which is commonly produced by copolymerizing PHB with hydroxyvalerate (HV), has been shown to improve the thermal processability, impact strength, and elongation-to-break of PHB without sacrificing its biodegradability [3]. Both PHB and PHBV have demonstrated comparable mechanical and durability properties to isotactic polypropylene [4], have proven to be suited for both injection- and blow-mold processes, and have exhibited acceptable performance as thermoplastic matrices in natural fiber composite applications [5–8]. At the end of their useful lives, conventional polyolefin-derived plastics and composites generally lie recalcitrant in landfills. These recalcitrant materials can potentially be replaced by fully biobased composite materials such as those studied herein that have been shown to rapidly biodegrade in anaerobic landfills [9], seawater, and compost environments.

In comparison to synthetic fillers, natural-fiber lignocelluloses offer advantages of low cost, biodegradability, rapid renewability, low density, global availability, and good thermal and mechanical properties, including high specific stiffness and strength. Recycled wood waste in the form of sawdust and wood flour (WF) is among the most common lignocellulosic fillers for petroleum-based

* Corresponding author. Tel.: +1 650 723 4125; fax: +1 650 723 7514.
E-mail address: wsrubar@stanford.edu (W.V. Srubar).

0032-3861/$ – see front matter © 2012 Elsevier Ltd. All rights reserved.
doi:10.1016/j.polymer.2012.03.036

thermoplastics (e.g., polypropylene) in conventional wood-polymer composite (WPC) systems. WPCs are used in both temporary and permanent construction applications as durable, low-maintenance material replacements for wood and wood-based products.

Despite the notable advantages of natural fibers, lignocellulosic materials like wood flour (WF) possess a distinct disadvantage, namely, an undesirable hydrophilicity ascribed by the abundance of hydroxyl groups (-OH) present in cellulose and hemicellulose. The induced chemical potential between the accessible hydroxyls and polar water molecules produces an affinity for hydrogen bond formation. Bound water in the lignocellulose leads to the separation of cellulose fibrils and hydroexpansion of the wood cell wall, causing several adverse effects on WPC mechanical and durability properties. Such effects include stiffness and strength reductions, dimensional instability, matrix cracking, and potential mass loss. The presence of moisture also provides the necessary conditions for in-service biodeterioration due to the invasion of fungal and microbial species. To counter the propensity for lignocellulose to absorb moisture and to address the surface energy incompatibility between hydrophobic polyolefin matrices and hydrophilic natural fillers, chemical coupling agents such as isocyanate, silane, methylmethacrylate (MMA), acrylonitrile, and maleic anhydride (MA) have been used in natural fiber composite systems and have been shown to increase fiber hydrophobicity and wettability, as well as improve fiber-matrix interfacial adhesion. A thorough summary on the physical fiber modifications and fiber-matrix chemical compatibilization techniques for natural fiber reinforced plastics and their characterization methods can be found in [10].

Whether or not the individual composite constituents are chemically modified, WPCs used in outdoor applications are inevitably exposed to transient and oftentimes harsh and severely fluctuating hydro- and hygrothermal environments. In outdoor applications, dimensional stability of WPCs is critical to the preservation of mechanical integrity and material durability. Thus, knowledge of the underlying mechanisms that govern moisture ingress, development of theoretical models to describe the kinetics of water transport, and quantification of the efficacy of chemical modifications are essential for evaluating treatment alternatives, for estimating service life, and for predicting long-term composite material performance.

Previous studies have successfully applied diffusion theory-based models to characterize the water absorption processes of WPCs with both virgin [11–14] and recycled [15,16] polyolefin matrices. However, studies of water transport kinetics and moisture-induced thickness swelling in WF-reinforced biopolymeric composites are quite limited. Anderson [17] investigated the water absorption behavior of WF/PHB composites and found that maleic anhydride reduced the initial rate of water uptake and increased time to damage initiation. Almgren et al. [18] studied the effect of butantetracarboxylic acid (BTCA) on thickness swelling and diffusion in WF/PLA composites, concluding that BTCA effectively reduced hydroexpansion and preserved dimensional stability of the composites.

The objectives of this work were to evaluate the governing kinetic diffusion behavior and model the time-dependent water transport processes of WF/PHBV biopolymeric composites exposed to various hydrothermal environments, as well as to demonstrate that the transport properties of environmentally benign composites are comparable to those of petroleum-based WPCs. A novel predictive model for determining the equilibrium moisture content (EMC) of both biopolymer and petroleum-based polymer wood-flour composites is proposed and validated with both presented and cited experimental results. The thermodynamic Arrhenius rate-law dependency of the diffusion coefficients on temperature and filler volume fraction was investigated. Furthermore, the effectiveness of both a silane fiber treatment and a MA graft-copolymerization technique on inhibiting polymer and composite water uptake was evaluated through a comparison of water transport activation energies and plots of composite isodiffusion. Finally, dimensional stability of each composite formulation was assessed via determination of β, a moisture-induced hydro-expansion swelling coefficient correlated with WF weight percent and expressed in strain per total mass fraction of absorbed moisture.

2. Theoretical formulation

2.1. Mechanisms of water transport

The complex mechanisms that influence the kinetics of water transport in WPC systems depend on the matrix-polymer molecular structure (e.g., polar groups, crosslink density, crystallinity), lignocellulosic filler morphology, ambient moisture content, temperature, and the existence of any voids, flaws, and microcracks along the fiber-matrix interface. Numerous mechanisms may be active during the absorption process. Moisture transport in WPCs is dominated by: 1) diffusion of water molecules between polymer chains; 2) capillary transport of liquid water into voids, microcracks, and interfacial gaps that exist due to poor fiber wettability; and 3) sorption by the filler due to a chemical potential gradient induced by the profusion of hydroxyls in lignocellulose. Despite concurrent mechanisms, the overall process can be classified and characterized using mathematical models based on polymer diffusion theory [11].

Water transport behavior in a polymer system can be classified into one of three cases: Fickian diffusion (Case I), polymer relaxation-controlled diffusion (Case II), and anomalous (non-Fickian) diffusion. The governing case can be distinguished theoretically via determination of the rate constants n and k in the following equation from the shape of the experimental sorption curve:

$$\frac{M_t}{M_\infty} = kt^n \tag{1}$$

where M_t and M_∞ are the moisture content (%) at a given time, t, and the EMC (%), respectively. The kinetic behavior is considered Fickian when $n = 0.5$, relaxation-controlled when $n = 1$, or anomalous when $0.5 < n < 1$. The kinetic processes of water absorption in lignocellulose-reinforced thermoplastics typically exhibit Fickian diffusion behavior [19].

2.2. Fick's laws and diffusion coefficients

Analogous to Fourier heat transfer theory, Fick's laws of molecular diffusion were formulated based on random-walk mass transfer, where the rate or flux of mass transport, J, is proportional to the gradient of molecular concentration, C, parallel to the direction, x, of diffusion:

$$J = -D\frac{\partial C}{\partial x} \tag{2}$$

where the proportionality constant, D, is the diffusion coefficient. The negative sign indicates molecular motion from high to low concentrations. Eq. (2) is known as Fick's First Law of Diffusion for steady-state transport. Considering the conservation of mass for the case of non-steady-state transport and constant D, the governing equation for one-dimensional mass transfer in an isotropic medium can be expressed by Fick's Second Law of Diffusion:

$$\frac{\partial C}{\partial t} = -D\frac{\partial^2 C}{\partial x^2} \tag{3}$$

With further assumptions that a) the material medium is homogeneous, b) the diffusion process occurs in a thin sheet such that all mass is transferred through the planar faces and a negligible amount is transported through the edges, c) the moisture boundary conditions are constant, and d) the material has an initially uniform moisture concentration profile, the analytical solution to Eq. (3) for a plane sheet of thickness, h, can be expressed as [20]:

$$\frac{M_t}{M_\infty} = 1 - \frac{8}{\pi^2}\sum_{n=1}^{\infty}\frac{1}{(2n-1)}\exp\left[-\frac{D(2n-1)^2\pi^2 t}{h^2}\right] \tag{4}$$

The Fickian diffusion coefficient, D, is the most important parameter in the Fickian diffusion model as it quantifies the ability of solvent molecules to penetrate the composite material. It can be calculated using the following equation:

$$D_A = \frac{\pi}{16}\frac{h^2\theta^2}{M_\infty^2} \tag{5}$$

where D_A is the apparent diffusion coefficient, and θ is the initial linear slope of the experimental sorption curve:

$$\theta = \frac{M_2 - M_1}{\sqrt{t_2} - \sqrt{t_1}} \tag{6}$$

If the specimen dimensions satisfy the thin-sheet assumption, D_A is synonymous with the one-dimensional Fickian diffusion coefficient, D; else, an edge correction factor (ECF) must be applied to correctly determine D. For the disc specimens of radius, r, and thickness, h, studied herein [21]:

$$D = D_A\left[1 + \frac{h}{r}\right]^{-2} \tag{7}$$

It should be noted that the ECF, which is defined as the positive square of the quantity in brackets, reduces to unity for a plane sheet with $h << r$.

2.3. Thermodynamics of water transport

The increased mobility of both solvent and solute molecules at higher temperatures further activates the transport mechanisms that govern Fickian diffusion. Thus, the Fickian diffusion coefficient characteristically exhibits an Arrhenius rate law temperature dependence:

$$D = D_0\, exp\left(-\frac{E_a}{RT}\right) \tag{8}$$

where D_0 is the permeability index (m^2/s), E_a is the activation energy (J/mol) of the diffusion process, R is the universal gas constant (8.3145 J/mol-K), and T is the absolute temperature (K).

3. Materials and experimental methods

3.1. Materials

PHBV (ENMAT™ Y1000P) was obtained from Tianan Biological Materials Company in a pelletized form suitable for injection molding. 20-mesh oak WF (2037-Oak) was supplied by American Wood Fibers, Schofield, Wisconsin, USA. A fiber sieve analysis confirmed a monodisperse particle size <841 μm. For the silane treatment and MA reactive extrusion, trimethoxy(octadecyl)-silane (C21H46O3Si), MA (2.5-Furandione, C4H2O3) (stored under vacuum), dicumyl peroxide (bis(1-methyl-1-phenylethyl) peroxide, C18H22O2), and phenolphthalein were obtained from Sigma–Aldrich.

3.2. Test specimen manufacture

Complete details of the silane-fiber thermochemical vapor deposition technique, MA reactive extrusion, compounding, and injection-mold processing can be found in [22]. Three families of WF/PHBV composites were fabricated. These families included neat PHBV/untreated WF (P), neat PHBV/silane-treated WF (PS), and 2% MA-treated PHBV (MA-PHBV)/untreated WF (2M). Specimen nomenclature was derived from composite family classification (P, PS, 2M) and the various target fiber loadings of 0%, 20%, and 40% by weight percent of filler. Due to the potential for error during composite manufacture, the actual WF constituent content was verified post-processing using a solvent dissolution method outlined in ASTM D3171 [23]. A list of all sample formulations, material constituents, and post-processing fiber weight percent can be found in Table 1. To illustrate the need for WF content verification, silanated and maleated composite specimens with 40% target filler weight percent had actual fiber loadings of 52% and 46%, respectively. The remaining composite formulations were more consistently manufactured with the intended fiber contents. Neat resin and composite disc test specimens with an approximate diameter of 50 mm and thickness of 3 mm were produced during the injection-molding process for the isothermal water sorption experiments.

3.3. Isothermal water absorption

To investigate the effect of temperature on the diffusivities of polymers and composites with varied WF weight percents and chemical treatments, isothermal water immersion studies were performed in accordance with ASTM D570-98 [24]. Three specimens of each sample were first conditioned at 103 ± 2 °C for 72 h in an environmental chamber, and sample mass loss was monitored to ensure a final oven-dry condition prior to immersion.

Sets of samples were submerged in airtight plastic containers filled with distilled water held constant at four different temperatures (4 °C, 15 °C, 21 °C, 37 °C) in controlled environmental chambers. Periodically, each specimen was taken from the water and subsequently weighed after its surface moisture was carefully removed with an absorbent cloth. The amount of time each sample was removed from the immersion was negligible compared to the time intervals between measurements. For each increment of time, the intermittent M_t was calculated for each sample:

$$M_t = \frac{m_t - m_o}{m_o} \times 100\% \tag{9}$$

where m_t and m_o are the sample mass after a given immersion time, t, and the oven-dry condition, respectively. Average moisture

Table 1
WF/PHBV composite formulations and actual constituent weight percents.

Specimen	Constituent material			
	Neat PHBV	Untreated WF	Silane-treated WF	MA-PHBV
P (PHBV)	100.0	–	–	–
P20	79.9	20.1	–	–
P40	60.0	40.0	–	–
P20S	78.0	–	22.0	–
P40S	48.1	–	51.9	–
2M (MA-PHBV)	–	–	–	100.0
2M20	–	20.6	–	79.4
2M40	–	46.0	–	54.0

contents for each sample were plotted versus square-root-time to obtain the experimental sorption curve. The samples were immersed until most samples achieved an equilibrium state (~4000 h) where a negligible change in sample mass was observed. Throughout the duration of the immersion tests, there was no evidence of biodeterioration initiated by foreign microbial or fungal species.

The highly crystalline and predominantly hydrophobic chemical nature of PHBV and the size of the sample discs together resulted in an exceptionally protracted sorption process for the neat polymer resin specimens. The initial slopes of water uptake were able to be determined; however, for modeling purposes, the equilibrium moisture contents (EMCs) need be characterized. To obtain the saturation values, the sorption process was expedited for PHBV and MA-PHBV, wherein three desiccated rectangular samples of dimension 2 mm × 6 mm × 30 mm were immersed in distilled water held at 95 ± 2 °C until equilibrium. The maximum moisture contents at complete saturation, which were assumed to be temperatureindependent for the thermal range used in this study, were found using Eq. (9).

3.4. Hydroexpansion

All water immersion disc specimens were marked with three points on the disc face (out-of-plane) and the disc edge (in-plane) for thickness and radial swelling measurements that were taken using a digital micrometer with an accuracy of 1 μm and calipers with an accuracy of 10 μm, respectively. To correlate hydroexpansion coefficients with total moisture content, thickness swelling, radial swelling, and moisture content measurements were taken concurrently. The equation to calculate dimensional change for both thickness and radial hydroexpansion is analogous to Eq. (9).

4. Results and discussion

4.1. Experimental sorption curves

The characteristic water absorption behavior of neat PHBV polymer and WF/PHBV composites is shown in Fig. 1 where total absorbed moisture, M_t (%), is plotted versus square-root-hours ($\sqrt{h}$) for PHBV and untreated composites hydrothermally conditioned at 37 °C.

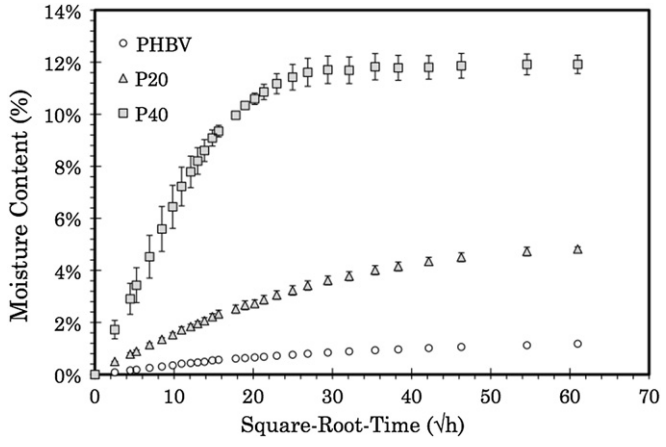

Fig. 1. Experimental sorption curves for neat PHBV and untreated WF/PHBV composite disc specimens at 37 °C. Weight gain measurements were made in triplicate. The error bars show the high and low moisture content values. Due to the small margin of error for PHBV and P20, the error bars are obscured from view.

4.1.1. Effect of WF filler

It can be seen from the figure that the neat PHBV polymer does absorb trace amounts of moisture; however, the relative hydrophilicity of the lignocellulose dominates the water sorption process of the composites. Expectedly, both the isothermal rates of water uptake and EMCs of the composites increase as the WF filler concentration increases. The moisture content of the P40 samples equilibrated at 11.9%. P20, which had yet to reach complete saturation, had a moisture content of 4.8% after 4000 h (63 $\sqrt{h}$) of immersion. Similar sorption curves were obtained for all untreated and treated WF composite samples in which an initially linear uptake region was followed by a gradual reduction in rate of absorption until equilibrium was reached.

The authors have previously reported that increasing the WF content from 0 to 40 vol% in PHBV can inhibit polymer crystallization as it cools from the melt, and the overall crystallinity of the matrix phase decreases approximately 16% from 58.4 to 49.1%. These data, which were obtained from DSC traces for the composites studied here, can be found in [22]. Yoon et al. [25] found that the maximum amount of water absorbed in semi-crystalline polymeric materials depends primarily on polymer crystallinity, as well-formed spherulites are inaccessible to moisture penetration. Thus, the increase in absorbed moisture with increasing WF could be attributed, in part, to the decreasing crystalline fraction of the PHBV matrix.

As will be further discussed in Section 4.3, the actual EMC and initial rate of water uptake varied for all samples depending on WF content and chemical treatment. Differences in isothermal environments significantly affected only the rate of transport, not the final EMC. Similar conclusions were reported in the literature for WF/PE composites [26].

Minor departures from the characteristic behavior were evident in a few of the P40, P40S, and 2M40 samples where expansion-induced cracking led to a slight increase (1–2%) in total moisture content after an initial equilibrium state. For subsequent diffusivity analyses, the EMCs of these samples were conservatively taken as the moisture content at the final equilibrium state. Furthermore, given the small sample error as shown by the error bars in Fig. 1, the following diffusivity analysis is based on an average experimental sorption curve for each formulation.

4.1.2. MA grafting and water absorption of PHBV

With the expedited sorption process for the neat polymer samples, PHBV and MA-PHBV achieved maximum moisture contents of 1.9% and 2.1%, respectively, substantiating the essentially hydrophobic nature of the highly crystalline polymers. It has been shown through calorimetry that, depending on the graft percent, the addition of MA functional groups on the PHBV backbone also slightly reduces the ability of the polymer to crystallize [22]. Thus, the small increase in the EMC of MA-PHBV versus neat PHBV can be attributed to a relative increase in the disordered, water-permeable amorphous material volume.

4.1.3. EMC: fiber saturation model for WPCs

While the specimens immersed at higher temperatures and those with higher WF contents reached equilibrium more rapidly than others, not all samples reached complete saturation after 4000 h of immersion. Premature experiment termination after a select number of days rather than allowing each sample to reach an ultimate equilibrium state would yield incorrect diffusion coefficients [27]. Therefore, in this study, where applicable, the EMCs of the samples obtained experimentally were used in classifying the diffusion behavior and in calculating the diffusion coefficient. However, for samples that had not yet reached equilibrium, an estimation of the EMC was calculated as per a proposed fiber saturation model for hydrophobic-polymer WPCs.

Studies have reported on the phenomenon by which the pre-processing WF density is increased after injection molding [28] and have attributed the mechanism to high processing pressures and either a) the collapse of the porous wood cell structure, or b) the injection of matrix material into wood fiber lumens, effectively reducing the filler to non-porous wood cell wall material [14,22]. It follows that the EMC of WF composite materials immersed in water can be predicted if the following assumptions are reasonable: 1) the matrix material is hydrophobic in nature; b) initial voids or microcracks in the material do not exist; and c) the material is considered saturated once the cell walls of the filler reach the wood cell wall fiber saturation point (FSP). The FSP is well-characterized to be 28–32% by oven-dry weight of wood and, while moderately dependent on ambient temperature, T, it is relatively independent of wood specie. The proposed fiber saturation model used to predict the EMCs of WF composites is:

$$M_\infty = w_f[0.3 - 0.001(T - 20)] \tag{10}$$

where the quantity in brackets is the equation for the FSP (%) [29] and w_f is the WF weight fraction (%). Fig. 2 shows the comparison of average EMCs of WF/PHBV composites obtained in this study and of WF/polyolefin and other predominantly hydrophobic-polymer composites published in the literature that reached complete saturation. As can be seen in Fig. 2, good agreement ($R^2 = 0.9169$) was found between the data and the predicted EMC values based on Eq. (10) using an ambient temperature of 21 °C. Fig. 2 also shows the bounds of the predicted EMC for the temperature range used in this study (4–37 °C).

While the fiber saturation model provides accurate estimates of equilibrium for WF/PHBV composites, slight deviations from the predictive model can occur if there is moisture-induced damage in the composite, if the fibers are treated, or if the matrix material is entirely hydrophobic, effectively encapsulating the hydrophilic WF filler. In the case of treated fibers, a modified fiber saturation point may be determined from a fiber soak test as conducted in [18] to quantify the maximum amount of absorbable moisture, provided that the fiber collapse mechanism during processing does not negate the effect of the treatment. It is also important to note that, while incremental absorbed moisture will cause the WF fibers to initially expand, the volumetric change may be inhibited due to the confinement of the polymer matrix. Although better dispersion and encapsulation of the wood particles by the plastic matrix has been shown to reduce moisture uptake [14], it is believed this phenomenon would most likely occur in lower WF-content WPCs where the fiber is heavily wetted by polymer. The proposed model assumes that the composite will eventually reach an equilibrium in which the fiber constituent is completely saturated – a conservative prediction that can be used to circumvent lengthy exposure tests for larger samples.

As an example application of the calculable EMC limit for a composite used in this study, Fig. 3 shows the relationship between the theoretical limit for equilibrium moisture and the P20 experimental 37 °C sorption data. It can be seen from a comparison of the curves that the sample moisture content approaches the theoretical limit as predicted by the fiber saturation model.

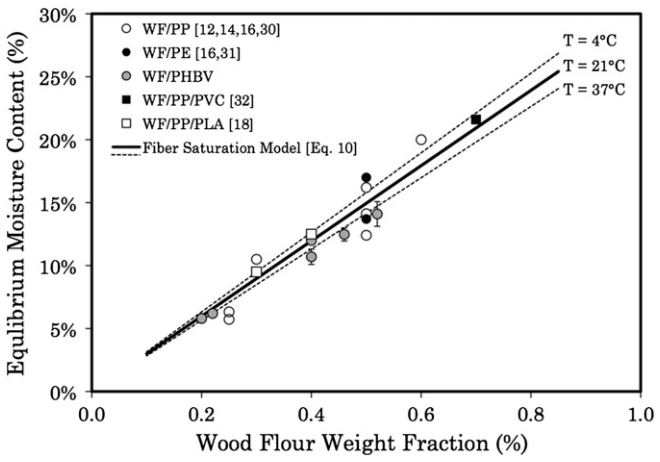

Fig. 2. Comparison between experimentally obtained EMCs in WPCs and predicted values using the fiber saturation model and an assumed ambient temperature of 21 °C [30–32].

4.2. Kinetics of water absorption

To investigate the governing diffusion behavior, an analysis of the kinetics of water absorption was performed via an empirical fit of the exponential model presented in Section 2.1 to the experimental sorption curves. A rearrangement of Eq. (1) yields:

$$\log\left(\frac{M_t}{M_\infty}\right) = \log(k) + n\log(t) \tag{11}$$

As an illustration of the analysis, Fig. 4 shows the experimental sorption data presented in Fig. 1 compared to the mathematical expression in Eq. (11). The values of the parametric constants n and k from the analysis are shown for each sample at all conditioning temperatures in Table 2. As can be determined from the collective values of n, the kinetic processes of water absorption approach the Fickian diffusion case, where $n \approx 0.5$, for all neat polymer and composite samples and for all thermal environments. At an immersion temperature of 37 °C, the values of the kinetic rate coefficient, n, ranged from 0.4233 to 0.5992 for all sample formulations. As water temperature approached freezing at 4 °C, the values of n decreased, reaching a minimum of 0.3668 in the 2M20 samples. Significant deviations from the Fickian diffusion case start to occur at values of $n \approx 0.17$, which would indicate the occurrence of a pseudo-Fickian transport phenomenon [20]. Given that all values of n obtained herein were greater than 0.3668, the theoretical formulations and rate constants based on Fick's Laws of Diffusion were considered valid modeling parameters for the transport of liquid water in WF/PHBV composites.

4.3. Diffusion coefficients

The Fickian diffusion coefficients for the neat polymer and composite samples were calculated according to the mathematical

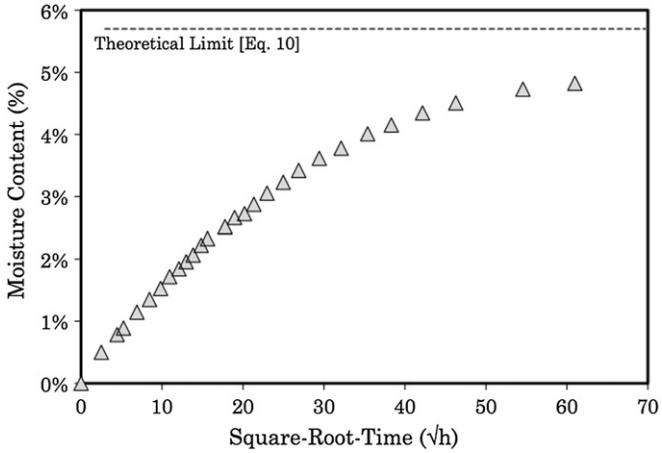

Fig. 3. Predicted equilibrium for the isothermal water absorption of P20 at 37 °C.

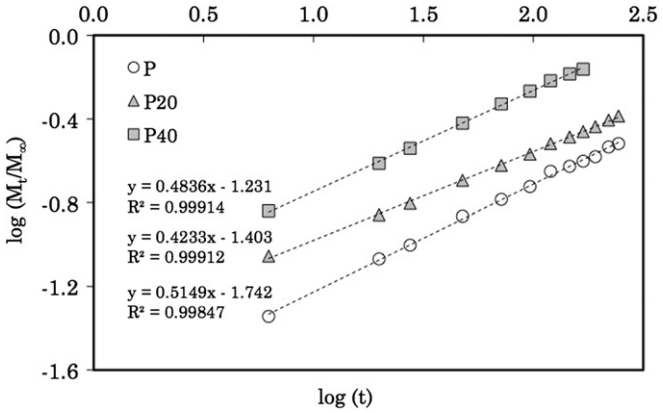

Fig. 4. Diffusion case analysis for untreated WF/PHBV composite samples conditioned at 37 °C.

expression in Section 2.2. The experimentally determined parameters used in the calculations, including the initial, linear slope of the sorption curve, θ, the least-squares regression value, R^2, for the linear measure of θ, the initial thickness of the sample, h_0, the initial diameter of the sample, d_0, and the EMC, M_∞, are included in Table 3, as well as the apparent diffusivity, D_A, the ECF for a disc geometry, and the calculated one-dimensional diffusion coefficient, D. The data presented were used to verify the adequacy of the Fickian diffusion model for plane sheet geometry. As Fig. 5 illustrates, the Fickian diffusion mathematical model derived in Section 2.2 can be used to accurately predict the time-dependent sorption for both 2M20 and 2M40 using the calculated diffusion coefficients. Similar results were obtained for all sample formulations.

Compared to neat polymer resins, the diffusivity of all composites increased with increasing WF content as expected, with a substantial increase in diffusion coefficient for the samples containing higher WF concentrations. As can be inferred from the values listed in Table 3, the diffusion coefficient for the ~40% filler content composites were higher by an order of magnitude compared to the ~20% WF samples. For example, at a temperature of 15 °C, $D = 0.30 \times 10^{-13}$ m^2/s, $D = 0.77 \times 10^{-13}$ m^2/s, and $D = 9.05 \times 10^{-13}$ m^2/s for P, P20, and P40, respectively. The diffusion coefficients also increased with temperature as demonstrated by the diffusivity of the P20 composites at 4 °C ($D = 0.38 \times 10^{-13}$ m^2/s) and at 37 °C ($D = 3.19 \times 10^{-13}$ m^2/s), suggesting a thermal rate dependency. This phenomenon is quantifiably explored in more detail in Section 4.4.

The diffusivity values obtained for WF/PHBV composites are comparable in magnitude to diffusion coefficients reported in WPC literature. Espert et al. [11] found similar trends with 10%, 20%, and 30% lignocellulose/polypropylene (PP) composites at two conditioning temperatures (23 °C and 50 °C), where the diffusion coefficient ranged from 1.67 to 16.4 $\times 10^{-13}$ m^2/s. Biodegradable PLA composites with 30% WF were reported to have a diffusivity of 15 $\times 10^{-13}$ m^2/s [18] at 23 °C. For high filler polyolefin composites, Najafi, et al. [16] found the diffusion coefficient to vary between 5.0 and 48.0 $\times 10^{-13}$ m^2/s for PP and polyethylene (PE) matrices reinforced with 50% WF. Similarly, Cheng, et al. [12] and Rangaraj and Smith [26] reported values of 31.0 $\times 10^{-13}$ and 58.0 $\times 10^{-13}$ for WF/polyolefin composites with filler weight fractions of 60% and 65%, respectively.

The increase in diffusivity for high WF content composites is attributed to the formation of an interconnected network of the permeable lignocellulose. The formation of this critical network depends on the reinforcing filler properties such as volume fraction, size and aspect ratio, fiber wettability, tendency to agglomerate, and partial, preferential, or random alignment of filler particles. The use of silane and MA coupling agents has been found to improve fiber wettability and particle dispersion, thereby inhibiting the formation of the critical fiber network and reducing the rate of water uptake in the resulting composites [13]. By a comparison of the composites with weight fraction of ~20% at 21 °C, the use of silane and MA lowered the diffusivity of the untreated specimen from 1.11 $\times 10^{-13}$ m^2/s to 0.90 $\times 10^{-13}$ m^2/s and 0.95 $\times 10^{-13}$ m^2/s, respectively. The results suggest that the chemical coupling agents reduced the hydrophilicity of the fibers either chemically via hydrolization of silane functional groups and/or physically by improving fiber dispersion in the hydrophobic matrix. Improved wettability also reduces the potential for microvoids to form at the fiber-matrix interface, effectively eliminating any discontinuities that may exacerbate initial rate of water uptake. Direct comparison could not be made between the P40, P40S, and 2M40 samples, as the actual weight fractions were 40.0%, 51.9%, and 46.0%, respectively. A more quantitative evaluation of the effectiveness of chemical coupling agents is presented in Section 4.5.

4.4. Thermodynamics of water transport

Diffusive water transport in materials is a thermally activated process as rises in temperature cause increased mobility of molecules. Accordingly, as discussed in the preceding section, all samples exhibited increased diffusivity at higher temperature conditions. The characterization of diffusion coefficients at various sorption isotherms permitted a quantitative thermodynamic analysis of the effect of temperature on water transport using the exponential Arrhenius model presented in Section 2.3.

Fig. 6 shows the Arrhenius plots for the three families of composites where the natural log of D is plotted against the inverse of *Temperature* (K^{-1}). The slope, m, and the intercept, b, from the linear regression analysis, as well as the determined Arrhenius rate constants E_a and D_0, the activation energy and the permeability index, respectively, are presented in Table 4. The linearity of the data obtained for each composite formulation substantiates the thermal rate-law dependence of the diffusion coefficient. The

Table 2
Governing diffusion case kinetic constants for all sorption isotherms.

Specimen	37 °C		21 °C		15 °C		4 °C	
	n	*k*	*n*	*k*	*n*	*k*	*n*	*k*
P	0.5149	0.0181	0.4223	0.0175	0.4431	0.0110	0.4005	0.0096
P20	0.4233	0.0395	0.3816	0.0302	0.3749	0.0261	0.3670	0.0197
P40	0.4836	0.0587	0.4387	0.0616	0.4561	0.0577	0.4357	0.0483
P20S	0.4923	0.0185	0.4557	0.0185	0.4706	0.0148	0.4443	0.0121
P40S	0.5992	0.0224	0.6013	0.0224	0.5377	0.0243	0.5109	0.0251
2M	0.5066	0.0130	0.4622	0.0130	0.4995	0.0102	0.4280	0.0083
2M20	0.4550	0.0189	0.4608	0.0189	0.4052	0.2515	0.3668	0.0203
2M40	0.5525	0.0318	0.5050	0.0318	0.4722	0.0297	0.4608	0.0290

Table 3
Fickian diffusion coefficients for WF/PHBV composites.

Specimen	T (K)	θ ($h^{-0.5}$)	R^2	h_0 (mm)	d_0 (mm)	M_∞ (%)	D_A ($m^2/s \times 10^{-13}$)	ECF	D ($m^2/s \times 10^{-13}$)
P	310	3.5E-04	0.990	3.30	49.7	1.9%	2.09	1.28	1.63
	294	2.1E-04	0.983	3.26	49.4	1.9%	0.77	1.28	0.60
	288	1.5E-04	0.986	3.21	49.6	1.9%	0.38	1.28	0.30
	277	9.7E-05	0.941	3.26	49.6	1.9%	0.16	1.28	0.12
P20	310	1.5E-03	0.991	3.19	49.7	5.7%*	4.07	1.27	3.19
	294	9.4E-04	0.957	3.22	49.7	6.0%*	1.41	1.28	1.11
	288	8.1E-04	0.943	3.21	49.7	6.1%*	0.98	1.28	0.77
	277	5.8E-04	0.922	3.23	49.7	6.2%*	0.49	1.28	0.38
P40	310	6.6E-03	1.000	3.24	49.9	11.9%	17.42	1.28	13.65
	294	4.8E-03	0.996	3.25	49.8	10.7%	11.89	1.28	9.31
	288	4.4E-03	0.998	3.25	49.9	9.9%	11.56	1.28	9.05
	277	3.4E-03	0.990	3.24	49.8	9.5%	7.43	1.28	5.82
P20S	310	1.7E-03	0.999	3.15	49.9	6.2%	3.82	1.27	3.01
	294	9.5E-04	0.999	3.15	49.8	6.6%*	1.14	1.27	0.90
	288	8.1E-04	0.996	3.14	49.9	6.7%*	0.79	1.27	0.62
	277	6.0E-04	0.995	3.16	49.8	7.0%*	0.41	1.27	0.32
P40S	310	8.9E-03	0.979	3.30	50.3	14.1%	23.98	1.28	18.73
	294	5.5E-03	0.964	3.36	50.3	13.3%	10.59	1.28	8.24
	288	4.6E-03	0.976	3.32	50.3	12.3%	8.36	1.28	6.53
	277	3.5E-03	0.969	3.31	50.3	11.9%	5.03	1.28	3.93
2M	310	4.3E-04	0.998	3.21	49.5	2.1%	2.39	1.28	1.87
	294	2.1E-04	0.996	3.23	49.3	2.1%	0.60	1.28	0.47
	288	1.6E-04	0.987	3.22	49.5	2.1%	0.35	1.28	0.28
	277	1.1E-04	0.985	3.21	49.5	2.1%	0.16	1.28	0.13
2M20	310	1.6E-03	0.997	3.07	49.7	5.8%	4.06	1.26	3.22
	294	9.4E-04	0.996	3.09	49.7	6.2%*	1.21	1.26	0.95
	288	7.9E-04	0.981	3.07	49.7	6.3%*	0.80	1.26	0.64
	277	5.8E-04	0.992	3.07	49.7	6.5%*	0.40	1.26	0.32
2M40	310	6.4E-03	0.994	3.34	50.2	12.5%	16.06	1.28	12.51
	294	4.1E-03	0.993	3.34	50.1	11.6%	7.56	1.28	5.89
	288	3.5E-03	0.982	3.35	50.1	11.5%	5.51	1.28	4.29
	277	2.8E-03	0.986	3.34	50.1	10.4%	4.35	1.28	3.39

*EMC predicted based on Eq. (10).

obtained rate constants allow for the determination of a composite Fickian diffusion coefficient for any isothermal water environment.

The relatively high activation energies of PHBV (56.5 kJ/mol) and MA-PHBV (58.9 kJ/mol), attributed to the highly crystalline, hydrophobic character of the semi-crystalline polymer, are comparable to other values reported in the literature for PHB copolymers with varying HV contents [33]. Expectedly, the activation energies for the neat polymers are less than the reported values of neat PHB (75 kJ/mol) [34]. PHBV and MA-PHBV are less crystalline than PHB, and the addition of HV reduces the energy needed for water to diffuse between polymer chain segments into more amorphous polymer regions. While increases in lignocellulose constituent content are accompanied by substantial reductions in activation energies of the neat polymers, the energies of WF/PHBV composites are an order of magnitude higher than those for polypropylene composites reinforced with kraft, coir, sisal, and luffa reported in the literature [11]. This suggests that some natural fillers like WF are more resistant to water uptake than other natural fibers when embedded in a polymer matrix.

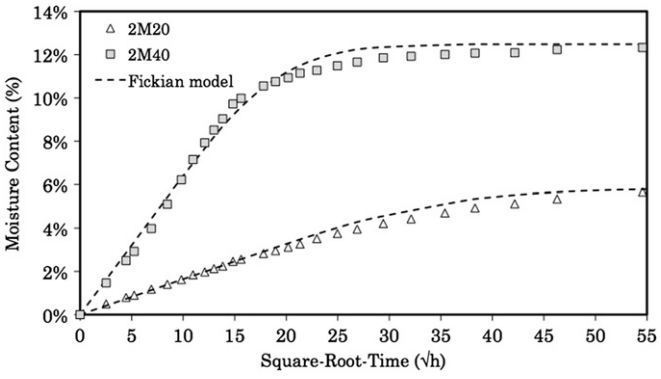

Fig. 5. Comparison of experimental data with Fickian diffusion model for MA-treated samples conditioned at 37 °C.

4.5. Effectiveness of chemical modifications

As discussed in Section 4.3, coupling agents act to improve moisture resistance of the WF, reducing composite diffusivity and impeding reductions in activation energy. While proper evaluations of chemical modifications on both the physical and mechanical properties of composites are necessary for assessing and comparing the effectiveness of chemical treatments, the differences in actual WF content make difficult the direct comparisons of determined parameters such as diffusion coefficients and activation energies between sample formulations.

To investigate the effectiveness of the silane and MA chemical modifications, the activation energy data shown in Table 4 is presented graphically in Fig. 7 to demonstrate the effect of WF content and chemical treatment on the water transport activation energies for the WF/PHBV composites. While all composite families exhibited a decrease in activation energy with increasing lignocellulose content, the activation energies for the untreated samples were significantly lower than the silane- and MA-treated composites. With better fiber wettability and fiber-matrix adhesion, the velocity of the transport process decreases. Other studies have concluded that improved fiber-matrix wettability and consolidation increase dimensional stability and moisture resistance [18]. Furthermore, it has been shown through microscopy that there are fewer gaps in the interfacial region of silane- and MA-treated WF/PHBV composites due to improved fiber wettability [22]. The coupling agents may also chemically block available hydroxyl groups from

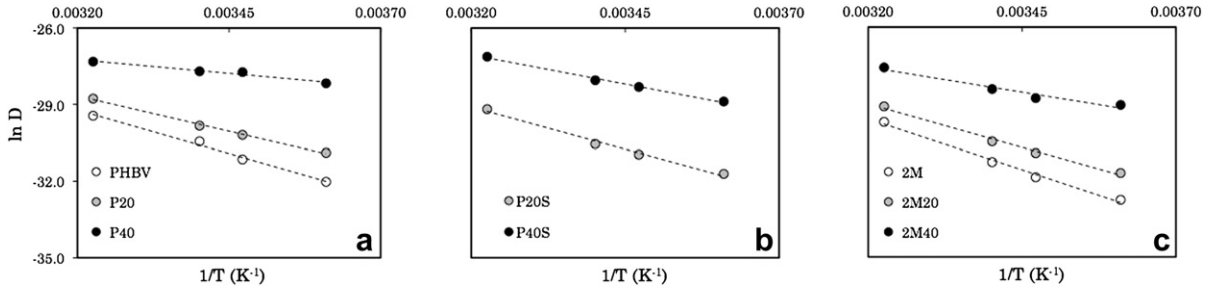

Fig. 6. Temperature-dependency and Arrhenius rate-law relationships for Fickian diffusion coefficients of a) untreated, b) silane-treated, and c) MA-treated WF/PHBV composites.

forming hydrogen bonds with water molecules, effectively retarding the diffusion process. However, the effect of this mechanism is believed to be minor in comparison to better wetting and dispersion, given that: 1) from the experimental sorption curves, only the rate of uptake, θ, was reduced, not the final EMCs; 2) only minor amounts of the coupling agents were used; and, 3) while the silane fiber treatment was a vapor deposition technique used to coat the fiber surface, WF fibers collapsed during processing, exposing accessible hydroxyls and providing direct pathways to the hydrophilic fiber regions [28].

The effects of chemical treatments can be quantified not only by the relative conservation of activation energies of the polymer with increasing WF filler as shown in Fig. 7, but also by the inhibition of mass transport and the corresponding reductions in the obtained Fickian diffusion coefficients. The effect of WF loading and temperature on the WF/PHBV diffusivity is presented in Fig. 8 for all three families of composites. As a baseline comparison, the coefficients for the untreated samples are presented in Fig. 8a, in which lines of isodiffusion have been extrapolated from experimental data. The results in Fig. 8b and c clearly demonstrate the effectiveness of the chemical modifications. The silane appears to effectively reduce the composite diffusivity at lower WF contents, perhaps due to improved fiber dispersion. However, as the lignocellulose filler percent increases, the benefits of dispersed fibers in the silane-treated samples are overcome as less matrix material is available to coat individual fibers. The diffusion coefficient was further reduced for all WF contents in the MA-treated samples. Espert et al. [11] concluded that greatest influence of moisture absorption behavior in WF thermoplastic composites aside from WF content is the degree of compatibilization between fibers and matrix. It follows that the MA-PHBV may be more effective in wetting the hydrophobic fiber than the silanation technique. Furthermore, from the resulting isodiffusion plots in Fig. 8, it can be concluded that, while there was no significant reduction in EMCs for the compatibilized samples, the chemical modifications, like traditional varnishes and coatings for wood [35], work to delay, not completely prevent, the kinetic transport of water into the bulk composite and that the combination of higher temperatures and higher WF contents work to counteract the treatments.

Lines of isodiffusion have the potential to serve as a WPC design tool given knowledge of the average ambient temperature and predicted service life for a given application. At an ambient temperature of 30 °C, untreated composites with a desired target diffusivity of 6.0×10^{-14} m^2/s must be fabricated with a target fiber loading of 28% by weight. In contrast, if the composites are treated with silane or MA, the fiber loading increases to 35% and 37%, respectively. Given the extremely low cost of wood flour, the ability to design composites with higher WF contents translates to both initial and maintenance cost savings over the predicted life of the material.

Table 4
Arrhenius rate constants.

Specimen	m	b	E_a (kJ/mol)	D_0 (m^2/s)
P	−6793	−7.48	56.48	5.63E-04
P20	−5512	−11.03	45.83	1.62E-05
P40	−2141	−20.39	17.80	1.39E-09
P20S	−5854	−10.03	48.67	4.43E-05
P40S	−4060	−13.95	33.76	8.76E-07
2M	−7087	−6.52	58.92	1.47E-03
2M20	−6038	−9.36	50.20	8.64E-05
2M40	−3483	−16.25	28.96	8.75E-08

4.6. Hydroexpansion coefficients

While the ability to achieve the same diffusivity with higher WF contents through chemical modification may have substantial environmental and economic benefit, the corresponding effects of additional amounts of lignocellulose on the material's mechanical and durability properties must be considered. The incorporation of WF and use of silane and MA as chemical coupling agents has been shown to substantially improve the mechanical properties of WF/PHA-based composites [11,17]. However, high fiber contents exacerbate dimensional stability issues associated with significant moisture-induced expansion of the WF.

To capture the effect of temperature and relative humidity on hydroexpansion of WF/polyolefin composites, Najafi, et al. [36] applied a thickness swelling rate model initially proposed by Shi and Gardener [37] that characterized the dimensional change during the moisture absorption process. The objective of the model is to characterize the time- and temperature-dependent hydroexpansion via determination of a swelling rate parameter for comparisons with wood. The model considered herein for moisture-induced mechanical strain first employed by Almgren et al. [38] utilizes an experimentally determined coefficient of

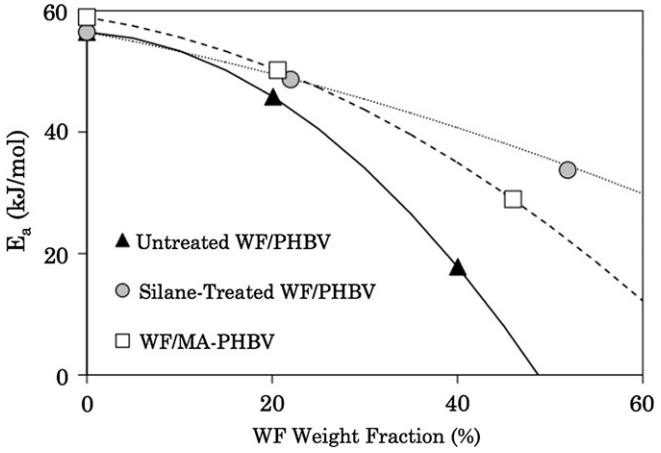

Fig. 7. Effect of lignocellulose content and chemical treatment on the water transport activation energy of PHBV.

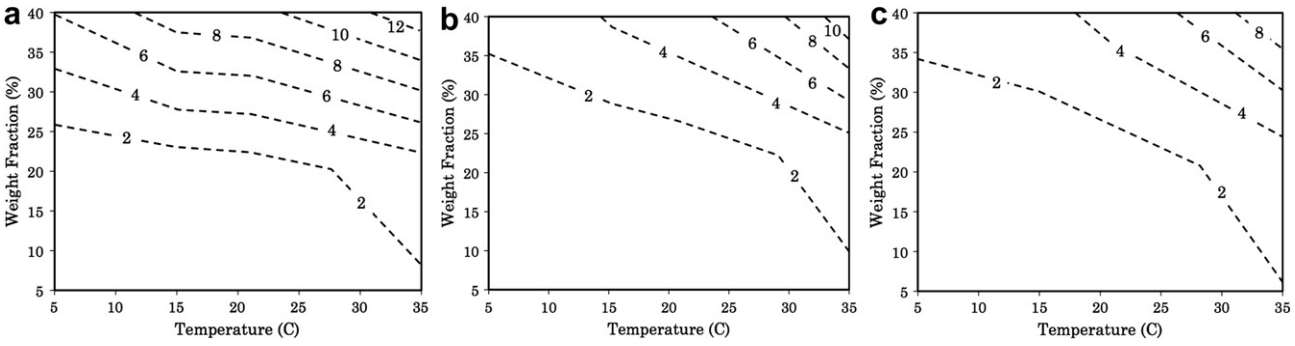

Fig. 8. Isodiffusion ($m^2/s \times 10^{-13}$) contours for a) untreated, b) silane-treated, and c) MA-treated composites.

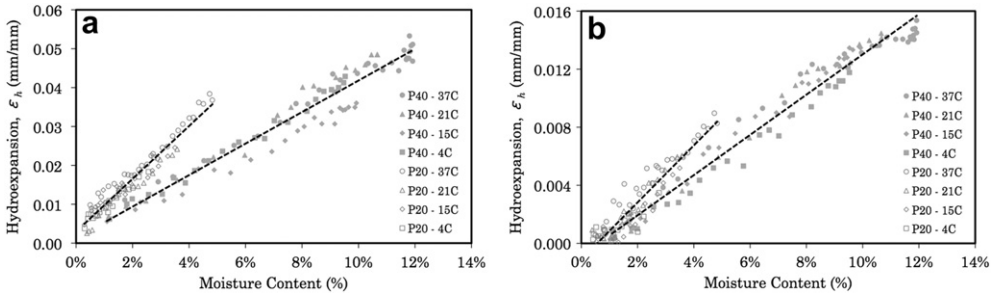

Fig. 9. Determination of coefficients of a) out-of-plane and b) in-plane hydroexpansion for thickness swelling of P20 and P40 WF/PHBV composites.

hydroexpansion, β, that is dependent on moisture content but independent of time and temperature. Assuming a homogenous, isotropic medium, the dimensional change (strain) cased by hydroexpansion of WPCs can be described by the following equation:

$$\varepsilon_h = \frac{\Delta h}{h_0} = \beta \times M_t \tag{12}$$

where ε_h is the hydrostrain (%/%) and Δh and h_0 are the change in out-of-plane thickness and original thickness of the composite disc specimen, respectively. A similar expression can also be used to obtain the in-plane radial swelling coefficient.

As shown in Fig. 9 for the P20 and P40 samples immersed at all four isotherms, the concomitant change in thickness and radial dimension measurements were correlated with total absorbed moisture throughout the isothermal sorption process for each composite sample. Values for β, calculated as the relative slope of the linear expansion ($\Delta\varepsilon_h/\Delta M_t$), were found to be independent of temperature for the different sorption experiments. The out-of-plane (thickness) coefficients (Fig. 9a) of linear hydroexpansion for P20 and P40 were determined to be 0.6789 and 0.4055, respectively, while the in-plane (radial) coefficients (Fig. 9b) were found to be 0.1964 and 0.1386. Similar in-plane and out-of-plane coefficients were determined for silane-treated and MA-treated composites. No expansion was evident in the neat PHBV and MA-PHBV polymer samples, thus their hydroexpansion coefficients were assumed to be zero.

Table 5
WF/PHBV composite maximum dimensional change and hydroexpansion coefficients.

Specimen	Out-of-plane thickness swelling (%)	Hygroexpansion coefficient, $\beta_t(\varepsilon/M_t)$	In-plane radial swelling (%)	Hygroexpansion coefficient $\beta_r(\varepsilon/M_t)$
P20	3.8%	0.6789	0.9%	0.1964
P40	5.3%	0.4055	1.5%	0.1386
P20S	5.1%	0.7898	1.0%	0.1643
P40S	10.2%	0.5207	2.5%	0.1882
2M20	4.4%	0.6268	0.9%	0.1788
2M40	6.6%	0.4892	1.9%	0.1598

The maximum out-of-plane and in-plane dimensional changes and hydroexpansion coefficients for all composite formulations are presented in Table 5. As expected, the most swelling was observed in the composites with higher wood flour contents. In general, the coefficients of out-of-plane hydroexpansion for the ~20% wood flour composites were approximately twice that of the ~40% wood flour composites for each of the untreated, silane-treated, and MA-treated families at the same moisture contents. Considering the data presented in Fig. 9a, the hydrostrain associated with 4% moisture content was 2.7% and 1.6% for P20 and P40, respectively.

Higher values for thickness swelling and hydroexpansion were obtained in the out-of-plane direction due to the in-plane random orientation of WF particles in injection-molded thermoplastic composites [38]. For example, as shown in Table 5, 2M20 samples swelled 4.4% out-of-plane and only 0.9% in-plane. Similarly, 2M40 samples swelled 6.6% in the out-of-plane direction and 1.9% in the in-plane direction. Wood fibers exhibit higher swelling in the tangential and radial directions compared to the longitudinal direction along the axis of the fiber [18]. The combination of random in-plane alignment and circular geometry of the disc specimens caused reduced hydroexpansion in the radial direction.

5. Conclusions

The governing kinetic behavior of water transport in untreated, silane-treated, and MA-treated bacterial biopolyester WF composites was investigated via experimental water immersion at four different temperatures (4 °C, 15 °C, 21 °C, 37 °C). The absorption processes for all families of composites were found to exhibit Fickian diffusion behavior. The equilibrium moisture content of WF/PHBV composites was predicted by a fiber saturation model in which equilibrium is defined as the weight fraction of the hydrophilic WF filler at its fiber saturation point. The Fickian diffusion

coefficients obtained for all samples exhibited a temperature-dependency as expressed by an Arrhenius rate law. The diffusion coefficients were found to be comparable in magnitude to conventional polyolefin-based WPC composites. A comparison of activation energies substantiated improved resistance to moisture uptake for the silane- and MA-treated composites in contrast to the untreated samples. The silane-treated fibers incurred damage via cell wall collapse during the injection-mold process. Thus, the improvement in hydrophobicity is attributed to better wettability and dispersion of fibers in the PHBV matrix. Isodiffusion plots were developed and presented to aid in the visualization of the dependence of composite diffusivity on temperature and fiber content and to allow direct assessment of the effectiveness of various chemical treatments in reducing composite diffusivity.

Both transverse and radial hydroexpansion coefficients were determined from the linear rate of incremental dimensional swelling per increase in moisture content and were found to be independent of temperature. Higher coefficients were found in the out-of-plane versus direction due to random in-plane orientation of fibers and in composites with lower lignocellulose contents.

Acknowledgments

The research presented herein was sponsored by the National Science Foundation (Grant CMMI-0900325), the California Environmental Protection Agency's Department of Toxic Substances Control (Grant No. 07T3451), and the NSF Graduate Research Fellowship Program. This body of work represents the views of the authors and not necessarily those of the sponsors. The collaboration with Dr. Srikanth Pilla, Prof. Joseph Greene at California State University – Chico, and Anthony Alvarado, Zachary C. Wright, and Olivia Isaac at Stanford University is gratefully acknowledged.

References

[1] Mohanty AK, Misra M, Drzal LT, editors. Natural fibers, biopolymers, and biobased composites. Boca Raton (FL): CRC Press, Taylor & Francis Group; 2005.
[2] Yu L, Dean K, Lin L. Prog Polym Sci 2006;31:576–602.
[3] Hakkarainen M. Adv Poly Sci 2002;157:113–38.
[4] Avella M, Martuscelli E, Raimo M. J Mat Sci 2000;35:523–45.
[5] Satyanarayana KG, Arizaga GGC, Wypych F. Prog Poly Sci 2009;34:982–1021.
[6] Christian, S.J. and S.L. Billington. ComP Part B;42(7):1920–1928.
[7] Wong S, Shanks R, Hodzik A. Macromol Mater Eng 2002;287:647–55.
[8] Dweib MA, Hu B, O'Donnell A, Shenton HW, Wool RP. Compos Struct 2004;63:147–57.
[9] Morse MC, Liao Q, Criddle CS, Frank CW. Polymer 2011;52(2):547–56.
[10] George J, Sreekala MS, Thomas S. Poly Eng Sci 2001;41(9):1471–85.
[11] Espert A, Vilaplana F, Karlsson S. Comp Part A 2004;35:1267–76.
[12] Cheng Q, Shaler S. Eur J Wood Prod; 2009:1–6.
[13] Wang W, Sain M, Cooper PA. Comp Sci Tech 2006;66:379–86.
[14] Steckel V, Clemons CM, Theomen H. J App Poly Sci 2007;103:752–63.
[15] Adhikary K, Pang S, Staiger MP. Chem Eng J 2008;142:190–8.
[16] Najafi SK, Kiaefar A, Hamidi E, Tajvidi M. J Reinf Plast Comp 2007;26(3):341–8.
[17] Anderson S. Ph.D. Dissertation. Washington State University, 2007.
[18] Almgren KM, Gamstedt EK, Berthold F, Lindstrom M. Poly Comp; 2009:1809–16.
[19] Islam MS, Pickering KL, Foreman NJ. J Polym Environ 2010;18:696–704.
[20] Crank J. The mathematics of diffusion. New York: Oxford UP; 1975.
[21] Marom GAD, Broutman LJ. Poly Comp 1981;2(3):132–6.
[22] Srubar WV, Pilla S, Wright ZC, Ryan CA, Greene JP, Frank CW, et al. Comp Sci Tech 2011;72:708–12.
[23] ASTM. West Conshohocken, PA: ASTM Intl; 2009.
[24] ASTM. West Conshohocken, PA: ASTM Intl; 1998.
[25] Yoon JS, Jung HW, Kim MN, Park ES. J Appl Polym Sci 2000;77:1716–22.
[26] Rangaraj SV, Smith LV. J Therm Comp Mat 2000;13:140–61.
[27] Marcovitch NE, Reboredo MM, Aranguren MI. Polymer 1999;40:7313–20.
[28] Clemons C. In: Xanthos M, editor. Functional fillers for plastics. Weinhelm: Wiley-VCH; 2005. p. 249–70.
[29] Saiu JF. Transport processes in wood. New York: Springer-Verlag; 1984. pp. 245.
[30] Nitz H, Reichert P, Romling H, Mulhaupt R. Macromol Mater Eng 2000;276:51–8.
[31] Kaboorani A, Englund KR. J Comp Mat 2010;45(13):1423–33.
[32] Shi SQ. Wood Sci Technol 2007;41:645–58.
[33] Tang CY, Chen DZ, Yue TM, Chan KC, Tsui CP, Yu PHF. Comp Sci Tech 2008;68:1927–34.
[34] Poley LH, da Silva MG, Vargas H, Siquiera MO, Sanchez R. Polímeros: Ciência e Tecnologia 2005;15(1):22–6.
[35] Simpson W, TenWolde A. Forest products Laboratory (FPL). Wood handbook—wood as an engineering material. Gen. Tech. Rep. FPL–GTR–113. Madison: U.S. Dept of Ag, Forest Service, FPL; 1999. pp. 463.
[36] Najafi SK, Kiaeifar A, Tajvidi M, Hamidinia E. Wood Sci Technol 2008;42:161–8.
[37] Shi SQ, Gardner DJ. Comp Part A 2006;37:1276–85.
[38] Almgren KM, Gamstedt EK, Varna J. Polym Comp; 2010:762–71.